Compensation of Cross Coupling in Multiple-Receiver Wireless Power Transfer Systems

Minfan Fu, *Member, IEEE,* Tong Zhang, Xinen Zhu, *Member, IEEE,*
Patrick Chi Kwong Luk, *Senior Member, IEEE,* Chengbin Ma, *Member, IEEE*

***Abstract*—Simultaneous wireless charging of multiple devices is a unique advantage of wireless power transfer (WPT). Meanwhile, the multiple-receiver configuration makes it more challenging to analyze and optimize the operation of the system. This paper aims at providing a general analysis on the multiple-receiver WPT systems and compensation for the influence of the cross coupling. A two-receiver WPT system is first investigated as an example. It shows that theoretically by having derived optimal load reactances the important system characteristics can be preserved such as the original system efficiency, input impedance, and power distribution when there is no cross coupling between receivers. The discussion is then extended to general multiple-receiver WPT systems with more than two receivers. Similar results are obtained that show the possibility of compensating the cross coupling by having the derived optimal load reactances. Finally, the theoretical analysis is validated by model-based calculation and final experiments using real two- and three-receiver systems.**

***Index Terms*—Wireless power transfer, multiple receivers, cross coupling, compensation, load reactances**

I. Introduction

Due to the increasing demand in charging of electronic devices (e.g. wearable devices, cellphones, tablets, laptop computers, and medical implant devices), there has been growing interest in the research and applications of the wireless power transfer (WPT) technologies. Simultaneous wireless charging of multiple devices by WPT offers a unique application advantage. However, it also presents more challenging analysis and optimization issues on the operation of the system. The receiving devices such as multiple wearable devices, cellphones, and tablets, may have very different size, position and orientation, load characteristic, power requirement. For the conventional one-receiver WPT system, a lot of work has been done on the modeling, analysis, optimization and control at both component and system levels. Examples of such efforts include the design of high efficiency power sources [1], [2]; modeling, analysis and optimized design of coupling systems [3]–[5]; tunable impedance matching [6], [7]; feedback-based optimal load control [8]–[10]; and system-level design and optimization [11]–[14].

On the other hand, less common multiple-receiver WPT systems have also attracted some research interests. Although there are some basic contributions reported in the literature, the key deficiency of the current research work in this area is the complete omission or use of highly simplistic models of the coupling effects between the coils, in particular the cross coupling among the receivers [15]–[25]. Initial discussions on the cross coupling and its compensation can be found in recent years. [26] discusses the potential to compensate the decrease in efficiency by resonant frequency tracking or retuning lumped capacitors when more receivers are added, with no further work subsequently reported in the literature. A frequency tracking method is proposed in [27], which is used in a multiple-transmitter multiple-receiver system. While the frequency tracking method could improve the overall performance, it cannot control the power delivered to each individual receiver and hence the associated efficiency. In [28], the impedance matching is proposed for individual loads to compensate the influence of cross coupling between the receivers, and the power distribution for a two-receiver system is discussed. However, the proposed model does not consider the effects of the parasitic resistances of the coils, resulting in overall system efficiency being overestimated. In [29] and [30], comprehensive discussions are provided on wireless power domino-resonator systems, i.e., multiple resonator systems, in which only a single resonator connects the load. Power analysis is carried out to investigate individual power flow paths and their interactions. The purpose of multiple relay resonators is to improve the transmission efficiency for "midrange" applications. A multiple-receiver system with a source coil, a transmitter, and multiple receivers is discussed in [31]. The optimal loads are determined considering the cross coupling between the source coil and the receivers rather than among the receivers. Several simplifications are also made such as identical receivers, same radial positions of the receivers, and neglect of source coil's parasite resistance. The work reported in [32] focuses on the optimal loads for a multiple-receiver system without cross coupling, and shows that the efficiency decreases with cross coupling. The solution for the decrease in efficiency is not given.

From the aforementioned review, it is evident that more research is highly desirable to address the issues of cross coupling effects in multi-receiver WPT systems in a more

Manuscript received June 23, 2015; revised October 29, 2015; accepted for publication January 4, 2016. P. C. K. Luk would like to acknowledge the support by the Top-Notch Foreign Specialist Program for his Visiting Professorship at Shanghai Jiao Tong University, to which part of this work related.

M. Fu, X. Zhu, and C. Ma are with University of Michigan-Shanghai Jiao Tong University Joint Institute, Shanghai Jiao Tong University, 800 Dongchuan Road, Shanghai 200240, P. R. China (e-mail: fuminfan@sjtu.edu.cn; zhuxinen@sjtu.edu.cn; chbma@sjtu.edu.cn). C. Ma is also with the School of Mechanical Engineering, Shanghai Jiao Tong University, Shanghai, China. T. Zhang is with lntel Asia-Pacific Research & Development Limited, No. 880 Zixing Road, Shanghai 200241, P. R. China (e-mail: tong.t.zhang@intel.com). P. C. K. Luk is with Electric Power & Drives Group, School of Engineering, Cranfield University, Cranfield MK43 0AL, United Kingdom (email: p.c.k.luk@cranfield.ac.uk).

comprehensive manner. It is envisaged that, in moving from laboratory systems towards real-world applications, the receiver coils will inevitably be put close together for a number of practical reasons including the size and costs of the overall system. Thus, it is all the more important to establish a design framework that warrants a higher degree of accuracy, when more transmitter-receiver configurations with various coil combinations will emerge in the near future. In order to provide a key step for the design framework, this paper aims at providing a general analysis of the multiple-receiver WPT systems and deriving a compensation for the influence of the cross coupling. In such systems, the receiving coils may have different sizes and coupling to the transmitting coil and the other receiving coils. The cross coupling effects are investigated using a two-receiver WPT system as an example. The parasitic resistances of the coils are included in order to accurately derive the load reactances. It shows that theoretically by having the optimal load reactances the important system characteristics can be preserved such as the original system efficiency, input impedance, and power distribution when there is no cross coupling between receivers. Then the discussion is extended to general multiple-receiver WPT systems with more than two receivers. Similar results are obtained that show the possibility of compensating the cross coupling by having the newly derived optimal load reactances. Finally, the theoretical analysis is validated by model-based calculation and final experiments using real two- and three-receiver systems.

II. Two-Receiver System

A. System Configuration

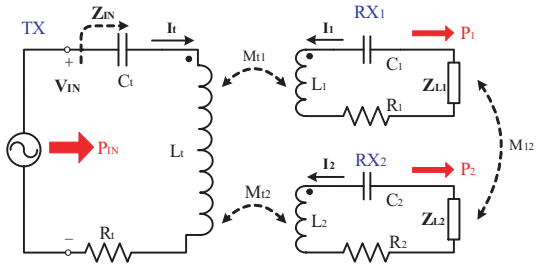

Fig. 1. A general two-receiver WPT system.

A general two-receiver WPT system is shown in Fig. 1. There are one transmitter (TX) and two receivers (RX_1 and RX_2). RX_1 and RX_2 are coupled to TX with mutual inductances of M_{t1} and M_{t2}, respectively. The mutual inductance between the two receivers is M_{12}. The coupling coefficient between any two coils is

$$k_{ij} = \frac{M_{ij}}{\sqrt{L_i L_j}}, \text{ for } i, j = t, 1, \text{or } 2. \tag{1}$$

L, C, and R with different subscripts (t, 1, or 2) represent the inductance, capacitance, and parasitic resistance of the corresponding coil. $\mathbf{Z_{L1}}$ and $\mathbf{Z_{L2}}$ are the loads for the two receivers,

$$\mathbf{Z_{Li}} = R_{Li} + jX_{Li}, \text{ for } i = 1, \text{or } 2, \tag{2}$$

where R_{Li} is the load resistance and X_{Li} is the load reactance. $\mathbf{Z_{RX1}}$ and $\mathbf{Z_{RX2}}$ are the equivalent impedances of the two receivers,

$$\mathbf{Z_{RXi}} = j\omega L_i + \frac{1}{j\omega C_i} + R_i + Z_{Li}, \text{ for } i = 1, \text{or } 2. \tag{3}$$

In the circuit, $\mathbf{I_t}$, $\mathbf{I_1}$ and $\mathbf{I_2}$ are the currents of TX, RX_1 and RX_2, respectively; $\mathbf{V_{IN}}$ and P_{IN} are the input voltage and input power of TX; and P_1 and P_2 are the power delivered to the two loads, $\mathbf{Z_{L1}}$ and $\mathbf{Z_{L2}}$ [see Fig. 1]. Finally, the overall system efficiency can be obtained as

$$\eta = \frac{P_1 + P_2}{P_{IN}} = \frac{|\mathbf{I_1}|^2 R_{L1} + |\mathbf{I_2}|^2 R_{L2}}{Re\{\mathbf{V_{IN}} \mathbf{I_t}^*\}}, \tag{4}$$

where $Re\{*\}$ means the real part of a complex number.

B. Zero Cross Coupling

For a two-receiver system, if the distance between the receivers are sufficiently large, the cross coupling between them can be neglected, i.e., $M_{12} = 0$ [refer to section IV-B]. In the conventional analysis, Z_{Li} (=R_{Li}) is pure resistive, and the resonance is achieved under the condition of

$$Im\{\mathbf{Z_{RXi}}\} = j\omega L_i + \frac{1}{j\omega C_i} = 0, \text{ for } i = 1, \text{or } 2, \tag{5}$$

namely zero reflected reactances at the TX side. Here $Im\{*\}$ means the imaginary part of a complex number. Therefore, the resonance for transmitter is achieved by

$$Im\{\mathbf{Z_{IN}}\} = j\omega L_t + \frac{1}{j\omega C_t} = 0. \tag{6}$$

Then under resonance, the relationships between the input voltage $\mathbf{V_{IN}}$ and the currents, $\mathbf{I_t}$, $\mathbf{I_1}$, and $\mathbf{I_2}$, can be described following the Kirchhoff's Voltage Law (KVL),

$$\begin{bmatrix} \mathbf{V_{IN}} \\ 0 \\ 0 \end{bmatrix} = \begin{bmatrix} R_t & j\omega M_{t1} & j\omega M_{t2} \\ j\omega M_{t1} & R_1 + R_{L1} & 0 \\ j\omega M_{t2} & 0 & R_2 + R_{L2} \end{bmatrix} \begin{bmatrix} \mathbf{I_t} \\ \mathbf{I_1} \\ \mathbf{I_2} \end{bmatrix}. \tag{7}$$

Solving (7) gives

$$\begin{cases} \mathbf{I_1} = \frac{-j\omega M_{t1} \mathbf{I_t}}{R_1 + R_{L1}} \\ \mathbf{I_2} = \frac{-j\omega M_{t2} \mathbf{I_t}}{R_2 + R_{L2}} \\ \mathbf{V_{IN}} = (R_t + \frac{\omega^2 M_{t1}^2}{R_1 + R_{L1}} + \frac{\omega^2 M_{t2}^2}{R_2 + R_{L2}}) \mathbf{I_t} \end{cases} \tag{8}$$

With these relationships, the input impedance is [see Fig. 1]

$$\mathbf{Z_{IN}} = \frac{\mathbf{V_{IN}}}{\mathbf{I_t}} = R_t + \frac{\omega^2 M_{t1}^2}{R_1 + R_{L1}} + \frac{\omega^2 M_{t2}^2}{R_2 + R_{L2}}, \tag{9}$$

the system efficiency is

$$\eta = \frac{\frac{\omega^2 M_{t1}^2 R_{L1}}{(R_1 + R_{L1})^2} + \frac{\omega^2 M_{t2}^2 R_{L2}}{(R_2 + R_{L2})^2}}{\mathbf{Z_{IN}}}, \tag{10}$$

and the power received by RX_i is

$$P_i = |\mathbf{I_t}|^2 \frac{\omega^2 M_{ti}^2 R_{Li}}{(R_i + R_{Li})^2}, \text{ for } i = 1, \text{or } 2. \tag{11}$$

Thus the power division ratio between the two receivers can be derived,

$$P_1 : P_2 = \frac{M_{t1}^2 R_{L1}}{(R_1 + R_{L1})^2} : \frac{M_{t2}^2 R_{L2}}{(R_2 + R_{L2})^2}. \tag{12}$$

From the above discussion, it can be seen that a two-receiver system with zero cross coupling has the following advantages. First for an individual coil the selection of the resonance capacitor only depends on its own inductance. And $\mathbf{Z_{IN}}$ is naturally pure resistive under the resonance. Therefore, complicated compensation for the coils is not needed. In addition, the power received by a single receiver is not affected by the other receiver when a constant current source is applied, i.e., I_t here. Theoretically, arbitrary power division ratios can be achieved according to (12). This decoupling of the receivers simplifies the analysis of the power transfer characteristics, and makes it straightforward to design and control the system.

C. Compensation of Cross Coupling

When two receivers are close to each other, the cross coupling between them will become obvious and affect the power transfer characteristics. With the original capacitors in (5) and (6), the relationships between the input voltage and the currents become

$$\begin{bmatrix} \mathbf{V_{IN}} \\ 0 \\ 0 \end{bmatrix} = \begin{bmatrix} R_t & j\omega M_{t1} & j\omega M_{t2} \\ +j\omega M_{t1} & R_1+R_{L1} & j\omega M_{12} \\ j\omega M_{t2} & j\omega M_{12} & R_2+R_{L2} \end{bmatrix} \begin{bmatrix} \mathbf{I_t} \\ \mathbf{I_1} \\ \mathbf{I_2} \end{bmatrix}. \tag{13}$$

Note here M_{12} is non-zero. Solving (13) gives

$$\begin{cases} \mathbf{I_1} = -\frac{\omega^2 M_{t2}M_{12}+j\omega M_{t1}(R_{L2}+R_2)}{\omega^2 M_{12}^2+(R_{L1}+R_1)(R_{L2}+R_2)}\mathbf{I_t} \\ \mathbf{I_2} = -\frac{\omega^2 M_{t1}M_{12}+j\omega M_{t2}(R_{L1}+R_1)}{\omega^2 M_{12}^2+(R_{L1}+R_1)(R_{L2}+R_2)}\mathbf{I_t} \end{cases}. \tag{14}$$

Now the power received by RX_i is

$$P_i = |\mathbf{I_t}|^2 \frac{[\omega^4 M_{tj}^2 M_{ij}^2+\omega^2 M_{ti}^2(R_{Lj}+R_j)^2]R_{Li}}{[\omega^2 M_{ij}^2+(R_{Li}+R_i)(R_{Lj}+R_j)]^2}, \tag{15}$$

for i, j = 1 or 2 and $i \neq j$, and the power division ratio becomes

$$\frac{P_1}{P_2} = \frac{[\omega^2 M_{t2}^2 M_{12}^2 + M_{t1}^2(R_{L2}+R_2)^2]R_{L1}}{[\omega^2 M_{t1}^2 M_{12}^2 + M_{t2}^2(R_{L1}+R_1)^2]R_{L2}}. \tag{16}$$

The power distribution here is obviously more complicated because P_i depends on the characteristics of both receivers. Besides, the input impedance is not pure resistive as well. By taking (14) into the first row of (13), $\mathbf{Z_{IN}}$ can obtained,

$$\mathbf{Z_{IN}} = R_t + \frac{\omega^2 M_{t1}^2(R_{L2}+R_2)+\omega^2 M_{t2}^2(R_{L1}+R_1)}{\omega^2 M_{12}^2+(R_{L1}+R_1)(R_{L2}+R_2)} + j\frac{\omega^3 M_{t1}M_{t2}M_{12}}{\omega^2 M_{12}^2+(R_{L1}+R_1)(R_{L2}+R_2)}, \tag{17}$$

which is now an inductive one.

Since

$$\mathbf{Z_{IN}} = \frac{\mathbf{V_{IN}}}{\mathbf{I_t}}, \tag{18}$$

and

$$\eta = \frac{|\mathbf{I_1}|^2 R_{L1} + |\mathbf{I_2}|^2 R_{L2}}{Re\{\mathbf{V_{IN}}\mathbf{I_t}^*\}}, \tag{19}$$

$$P_1 : P_2 = |\mathbf{I_1}|^2 R_{L1} : |\mathbf{I_2}|^2 R_{L2}, \tag{20}$$

it means that if the two-receiver system has a same set of the currents $(\mathbf{I_t}, \mathbf{I_1}, \mathbf{I_2})$ and fixed R_{L1} and R_{L2}, its important characteristics, the input impedance, the system efficiency, and the power division ratio, will be identical whenever there is the cross coupling or not. This can be achieved using properly introduced load reactances. The voltage-current relationships are described in the following equation,

$$\begin{bmatrix} \mathbf{V_{IN}} \\ 0 \\ 0 \end{bmatrix} = \begin{bmatrix} R_t & j\omega M_{t1} & j\omega M_{t2} \\ j\omega M_{t1} & R_1+R_{L1}+jX_{L1}^* & j\omega M_{12} \\ j\omega M_{t2} & j\omega M_{12} & R_2+R_{L2}+jX_{L2}^* \end{bmatrix} \begin{bmatrix} \mathbf{I_t} \\ \mathbf{I_1} \\ \mathbf{I_2} \end{bmatrix}, \tag{21}$$

where X_{L1}^* and X_{L2}^* are the optimal load reactances. Solving for a same set of $(\mathbf{I_t}, \mathbf{I_1}, \mathbf{I_2})$ in (7) and (21) gives,

$$\begin{cases} X_{L1}^* = -\omega\frac{M_{12}M_{t2}(R_1+R_{L1})}{M_{t1}(R_2+R_{L2})} \\ X_{L2}^* = -\omega\frac{M_{12}M_{t1}(R_2+R_{L2})}{M_{t2}(R_1+R_{L1})} \end{cases} \tag{22}$$

With this combination of load reactances, the original system efficiency, input impedance, and power division ratio in (9), (10), and (12) can be well preserved. This makes the design and control of the multiple-receiver systems more predictable in a real environment. Note X_{L1}^* and X_{L2}^* can be implemented by tuning the capacitors of the receivers [refer to section IV-A]

III. Multiple-Receiver System

Here the previous findings are extended to general multiple-receiver WPT systems, as shown in Fig. 2. There are one transmitter TX and $n(>2)$ receivers RX_i $(i = 1, \ldots, n)$. Similarly, M_{ti} is the mutual inductance between TX and RX_i, and M_{ij} is the mutual inductance between RX_i and RX_j $(j = 1, \ldots, n)$. The coupling coefficient between any two coils, RX_i and RX_j, is

$$k_{ij} = \frac{M_{ij}}{\sqrt{L_i L_j}}, \text{ for } i, j = t, 1, 2, ..., n. \tag{23}$$

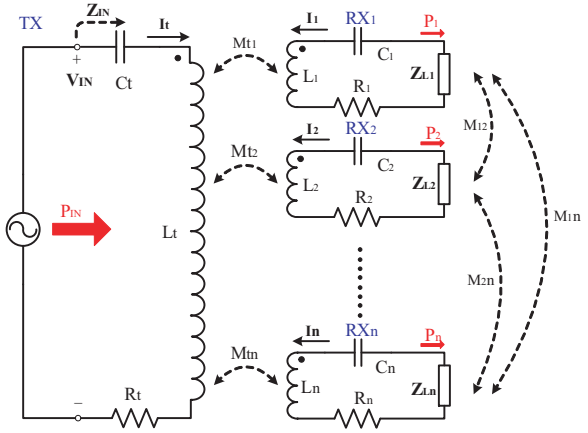

Fig. 2. The configuration of a multiple-receiver WPT system.

Again applying the Kirchhoff's Voltage Law (KVL) to the n-receiver system in Fig. 2, the current-voltage relationships can be obtained, as shown in (24) [refer to the following page]. Assuming zero cross coupling and pure resistive loads, i.e., $M_{ij} = 0$ and $X_{Li} = 0$, (24) can be further simplified to (25).

$$\begin{bmatrix} \mathbf{V_{IN}} \\ 0 \\ \vdots \\ 0 \\ 0 \end{bmatrix} = \begin{bmatrix} R_t & j\omega M_{t1} & \cdots & j\omega M_{t(n-1)} & j\omega M_{tn} \\ j\omega M_{t1} & R_1+\mathbf{Z_{L1}} & \cdots & j\omega M_{1(n-1)} & j\omega M_{1n} \\ \vdots & \vdots & \ddots & \vdots & \vdots \\ j\omega M_{t(n-1)} & j\omega M_{1(n-1)} & \cdots & R_{n-1}+\mathbf{Z_{L(n-1)}} & j\omega M_{(n-1)n} \\ j\omega M_{tn} & j\omega M_{1n} & \cdots & j\omega M_{(n-1)n} & R_n+\mathbf{Z_{Ln}} \end{bmatrix} \begin{bmatrix} \mathbf{I_t} \\ \mathbf{I_1} \\ \vdots \\ \mathbf{I_{n-1}} \\ \mathbf{I_n} \end{bmatrix}. \tag{24}$$

$$\begin{bmatrix} \mathbf{V_{IN}} \\ 0 \\ \vdots \\ 0 \\ 0 \end{bmatrix} = \begin{bmatrix} R_t & j\omega M_{t1} & \cdots & j\omega M_{t(n-1)} & j\omega M_{tn} \\ j\omega M_{t1} & R_1+R_{L1} & \cdots & 0 & 0 \\ \vdots & \vdots & \ddots & \vdots & \vdots \\ j\omega M_{t(n-1)} & 0 & \cdots & R_{n-1}+R_{L(n-1)} & 0 \\ j\omega M_{tn} & 0 & \cdots & 0 & R_n+R_{Ln} \end{bmatrix} \begin{bmatrix} \mathbf{I_t} \\ \mathbf{I_1} \\ \vdots \\ \mathbf{I_{n-1}} \\ \mathbf{I_n} \end{bmatrix}. \tag{25}$$

$$\begin{bmatrix} 0 \\ 0 \\ \vdots \\ 0 \\ 0 \end{bmatrix} = \begin{bmatrix} jX_{L1}^* & j\omega M_{12} & \cdots & j\omega M_{1(n-1)} & j\omega M_{1n} \\ j\omega M_{12} & jX_{L2}^* & \cdots & j\omega M_{2(n-1)} & j\omega M_{2n} \\ \vdots & \vdots & \ddots & \vdots & \vdots \\ j\omega M_{1(n-1)} & j\omega M_{2(n-1)} & \cdots & jX_{L(n-1)}^* & j\omega M_{(n-1)n} \\ j\omega M_{1n} & j\omega M_{2n} & \cdots & j\omega M_{(n-1)n} & jX_{Ln}^* \end{bmatrix} \begin{bmatrix} \mathbf{I_1} \\ \mathbf{I_2} \\ \vdots \\ \mathbf{I_{n-1}} \\ \mathbf{I_n} \end{bmatrix}. \tag{26}$$

Inspired by the previous analysis on the two-receiver system, it is reasonable to assume that the two systems described by (24) and (25) are able to achieve the same system characteristics. A sufficient condition for this assumption is that the currents, $\mathbf{I_t}, \mathbf{I_1}, \ldots, \mathbf{I_n}$, in (24) and (25) are identical. Then the optimal load reactances X_{Li}^*'s can be determined by letting (24) and (25) share a same solution of currents. Subtracting (25) on both sides of (24) gives (26). Thus X_{Li}^* can be solved as

$$X_{Li}^* = -\sum_{k=1,k\neq i}^{n} \frac{\omega M_{ik}\mathbf{I_k}}{\mathbf{I_i}}. \tag{27}$$

From (25) the relationship among the currents is

$$\mathbf{I_i} = -\frac{j\omega M_{ti}\mathbf{I_t}}{R_i+R_{Li}}. \tag{28}$$

Combining (27) and (28) gives

$$X_{Li}^* = -\sum_{k=1,k\neq i}^{n} \frac{\omega M_{ik}M_{tk}(R_i+R_{Li})}{M_{ti}(R_k+R_{Lk})}. \tag{29}$$

Note when n=2 (29) is identical with (22).

Originally complicated variations occur in the system efficiency, input impedance, and power division ratio when the cross coupling among the receivers becomes non-neglectable. With the derived optimal load reactances in (29), all the receivers can be treated as decoupled ones again. As same as in the two-receiver systems, the following important system characteristics can be preserved. Under the compensation, the overall system efficiency is

$$\eta = \frac{\sum_{i=1}^{n} \frac{\omega^2 M_{ti}^2 R_{Li}}{(R_i+R_{Li})^2}}{\mathbf{Z_{IN}}}; \tag{30}$$

The input impedance $\mathbf{Z_{IN}}$ is now pure resistive,

$$\mathbf{Z_{IN}} = R_t + \sum_{i=1}^{n} \frac{\omega^2 M_{ti}^2}{R_i+R_{Li}}; \tag{31}$$

and the power division ratio between two arbitrary receivers, RX_i and RX_j, is

$$P_i : P_j = \frac{M_{ti}^2 R_{Li}}{(R_i+R_{Li})^2} : \frac{M_{tj}^2 R_{Lj}}{(R_j+R_{Lj})^2}. \tag{32}$$

The derivation of (29) establishes a theoretical framework for the compensation of the cross coupling in the multiple-receiver WPT systems. It shows that the optimal load reactances depend on the load resistances, the parasitic resistances and relative positions (i.e., the mutual inductances) of coils. It is however noteworthy that in practice the required capacitances, i.e., the negative reactances in (29), may be difficult to obtain exactly by using discrete capacitors. In the following experiments the optimal load reactances are approximated through properly connecting multiple capacitors. Here, the focus is not on practical viability but rather on theoretical validation. Nonetheless, the experimental results show good agreements with the theoretical prediction, and thus validate the applicability of the proposed theoretical model. In the cases where there are uncertainties in parameters, particularly the loads and the couplings, additional communication and dynamic impedance matching networks would be required [33].

IV. Experimental Verification

A. Experimental Setup

As shown in Fig. 3, a four-port vector network analyzer (VNA), Agilent E5071C, is used for the measurement. Due to the limited number of the ports, a multi-receiver WPT system with at most three receivers was built and tested, i.e., port 1 for the transmitter (TX) and ports 2, 3, and 4 for the receivers ($RX_i,\ i=1,2,3$). All the coils are tuned to resonate at 13.56 MHz by using external series capacitors. The parameters and dimensions of the coils can be found in Table I and Fig. 4. The original load resistances for RX_i's, i.e., the input impedances

of the VNA ports here, are all standard 50 Ω ones (i.e., Z_{port} in Fig. 5(b)). As shown in Fig. 5, the required load reactances, X_{Li}'s, are realized by adjusting the capacitance of $C_i^{'}$, where

$$j\omega L_i + \frac{1}{j\omega C_i^{'}} = jX_{Li}, \text{ for } i = 1, 2, 3. \tag{33}$$

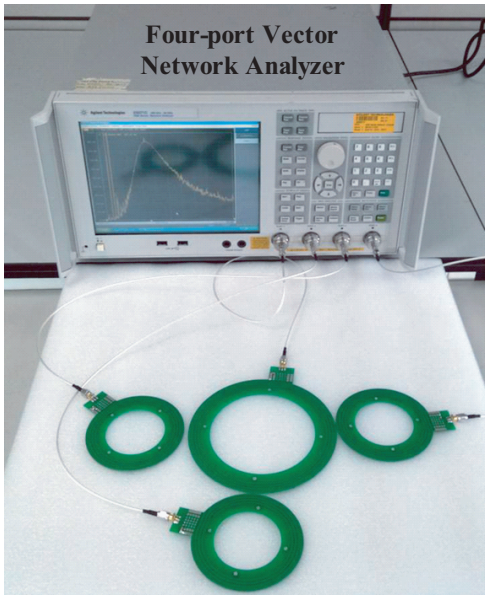

Fig. 3. An example of experimental setup

TABLE I
PARAMETERS OF COILS

Coils	Large coil	Small coil
Resistance (Ω)	4.78	1.28
Inductance (μH)	6.94	3.00

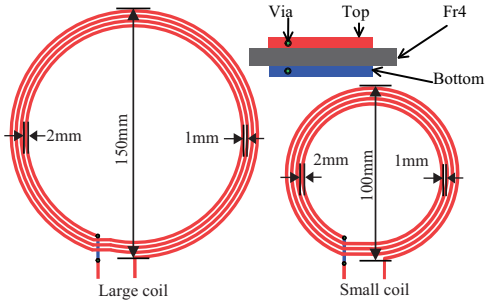

Fig. 4. Dimensions of the coils with different sizes.

In the experiments, a cylindrical coordinate system is introduced to describe the three-dimensional positions of the coils, as shown in Fig. 6. O_t is the center of the TX coil and the origin of the coordinates, i.e., (0,0,0). O_i ($i = 1, 2, 3$) is the center of the i-th RX coil. Its projection on the xy-plane is $O_i^{'}$. The coordinates of O_i are (r_i, θ_i, z_i), where r_i is the radial distance (length of $O_tO_i^{'}$), θ_i is the azimuth angle between $O_tO_i^{'}$ and x-axis, and z_i is the height (length of $O_iO_i^{'}$).

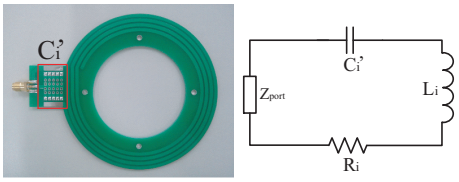

Fig. 5. Configuration of coils. (a) Photo. (b) Circuit model.

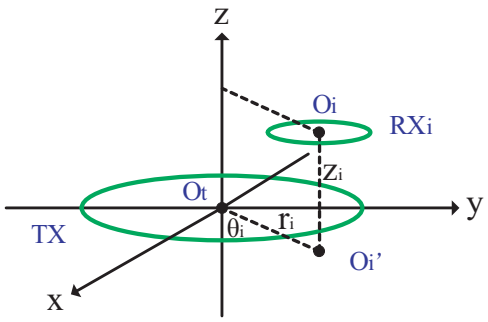

Fig. 6. The cylindrical coordination system for representing the three-dimensional coil positions.

B. Two-receiver System

As shown in Fig. 7(a), a two-receiver system is built, in which TX and RX_2 use the large coils and RX_1 uses the small one. In the experiments, TX and RX_2 are fixed at the positions of (0,0,0) and (150, π, -10), respectively. RX_1 moves from (125, 0, 0) to (125, π, 0) along a circle of radius 125 mm. Since the relative positions between the two receivers (RX_1 and RX_2) and TX keep constant, k_{t1}(=0.090) and k_{t2}(=0.066) are also constant during the movement of RX_1. k_{12} is measured by VNA and shown in Fig. 7 (b). At the beginning (i.e., θ_1 is around 0), k_{12} is small and neglectable. Then k_{12} is increasing with θ_1. Meanwhile, due to the cancellation of magnetic flux, there is a valley at $\theta_1 = \frac{3}{4\pi}$. At this particular position, the shared magnetic fluxes in opposite directions exactly cancel each other and lead to a zero cross coupling. In the experiments, the system efficiency is calculated as

$$\eta = \frac{|S_{21}|^2 + |S_{31}|^2}{1 - |S_{11}|^2}, \tag{34}$$

in which the S-parameters are measured by VNA. The the power division ratio is

$$P_1 : P_2 = |S_{21}|^2 : |S_{31}|^2, \tag{35}$$

and the input impedance, $\mathbf{Z_{IN}}$, can be directly read by VNA.

The comparison of the system efficiencies with/without the compensation of the cross coupling is shown in Fig. 8. Both the calculated (Cal) and experimental (Exp) results are given. Note the efficiencies are calculated using the circuit model. In the experiment, the worst-case efficiency (63%) occurs when RX_1 is rightly above RX_2 ($\theta_1 = \pi$), i.e., the position with the strongest cross coupling. The decrease in the efficiency can be effectively avoided by having the optimal load reactances. As shown in Fig. 8, the experimental and calculated efficiencies

TABLE II
INPUT IMPEDANCE AND POWER DIVISION RATIO IN TWO-RECEIVER SYSTEM

Position	$\theta_1 = 0$ (zero k_{12})		$\theta_1 = \pi$ (Uncompensated)		$\theta_1 = \pi$ (Compensated)	
Results	Calculation	Experiment	Calculation	Experiment	Calculation	Experiment
$\mathbf{Z_{IN}}$ (Ω)	$57.2 - j0$	$57.0 - j0.1$	$24.9 - j55.6$	$22.6 - j53.2$	$57.2 - j0$	$53.5 - j1.4$
$P_1 : P_2$	47.6% : 52.4%	46.9% : 53.1%	54.1% : 45.9%	53.2% : 46.8%	47.6% : 52.4%	47.2% : 52.8%

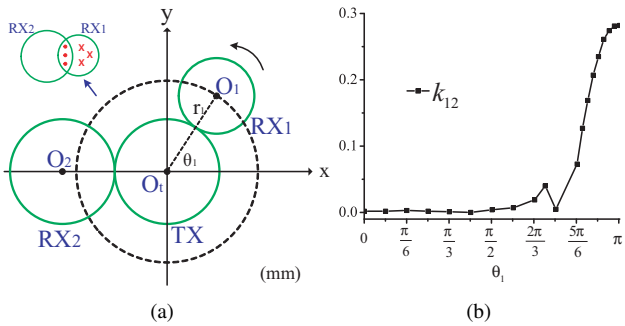

Fig. 7. Coil positions in the two-receiver system. (a) Top view. (b) k_{12} with a varying θ_1.

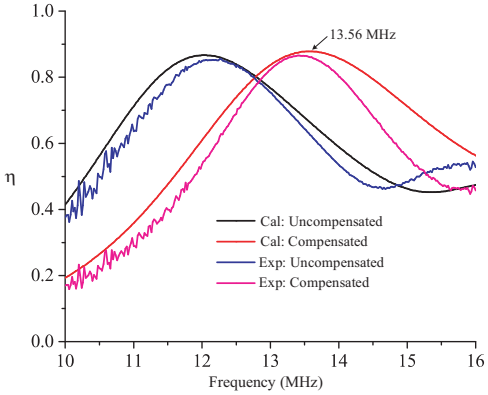

Fig. 9. Frequency responses of the two-receiver system at $\theta_1 = \pi$.

well match with each other for the both compensated and uncompensated systems. The small error is mainly caused by the unavoidable modelling error of the circuits and inaccuracy of the real capacitors. Under the compensation, the worst-case efficiency can be significantly improved from 63% to 86%, a similar level to the efficiencies when the cross coupling is neglectable. For reference purposes, the frequency responses with/without the compensation are compared at $\theta_1 = \pi$ in Fig. 9. Without the compensation, the shift of the resonance frequency is observed and the system efficiency decreases at the targeted 13.56 MHz. After applying the optimal load reactances, the resonance frequency is shifted back to 13.56 MHz. Thus the system efficiency is largely recovered. Mostly due to the frequency-dependant circuit parameters, there is error between the experimental and calculated results. Meanwhile, the results at the targeted frequency, 13.56 MHz, still show a reasonable accuracy.

Besides the avoidance of the efficiency drop, the proposed compensation is expected to maintain both the original input impedance $\mathbf{Z_{IN}}$ and power division ratio between the two receivers when there is the cross coupling. Here the results at $\theta_1 = 0$ and $\theta = \pi$ (the worst case) without/with compensation are shown and compared in Table II. As mentioned above, at $\theta_1 = 0$ k_{12} is small enough to be neglectable, i.e., the case with zero cross coupling; while at $\theta_1 = \pi$ $k_{12}(= 0.281)$ is maximized because RX_1 and RX_2 are overlapped. As shown by the results when the two-receiver system is uncompensated/compensated, the original characteristics of the system such as $\mathbf{Z_{IN}}$ and power division ratio $P_1 : P_2$ can be recovered even in the worst case, i.e., $\theta_1 = \pi$. Again the small error between the calculated and experimental results are caused by the unavoidable modelling error and the inaccuracy of real devices.

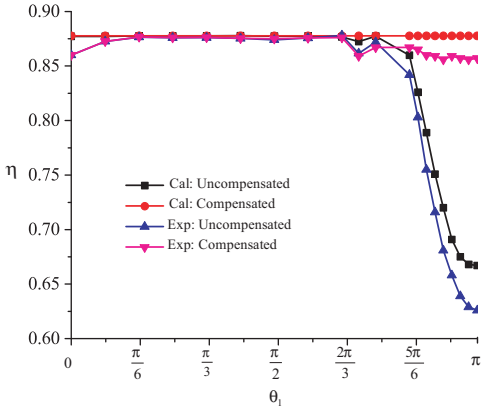

Fig. 8. Comparison of the system efficiencies in the two-receiver system.

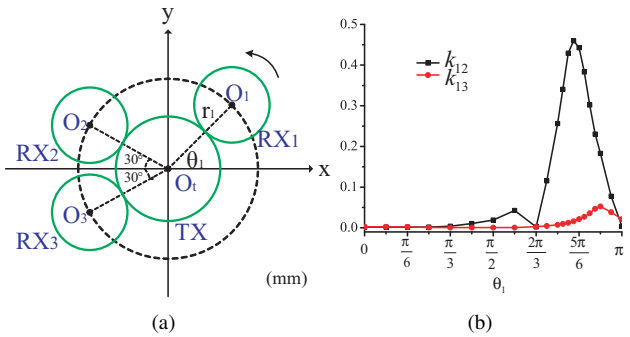

Fig. 10. Coil positions in the three-receiver system. (a) Top view. (b) k_{12} and k_{13} with a varying θ_1.

TABLE III
INPUT IMPEDANCE AND POWER DIVISION RATIO IN THREE-RECEIVER SYSTEM ($\theta_1 = 0$)

Position	$\theta_1 = 0$ (Uncompensated)		$\theta_1 = 0$ (Compensated)	
Results	Calculation	Experiment	Calculation	Experiment
$\mathbf{Z_{IN}}$ (Ω)	$51.1 - j0.6$	$52.5 - j1.6$	$51.3 - j0$	$52.5 - j0.4$
$P_1 : P_2 : P_3$	51.4% : 24.3% : 24.3%	48.4% : 26.2% : 25.4%	51.4% : 24.3% : 24.3%	49.5% : 25.6% : 24.9%

TABLE IV
INPUT IMPEDANCE AND POWER DIVISION RATIO IN THREE-RECEIVER SYSTEM ($\theta_1 = \frac{5\pi}{6}$)

Position	$\theta_1 = \frac{5\pi}{6}$ (Uncompensated)		$\theta_1 = \frac{5\pi}{6}$ (Compensated)	
Results	Calculation	Experiment	Calculation	Experiment
$\mathbf{Z_{IN}}$ (Ω)	$20.2 - j12.6$	$23.1 - j13.2$	$51.3 - j0$	$53.8 - j0.6$
$P_1 : P_2 : P_3$	14.7% : 24.4% : 60.9%	13.2% : 22.9% : 63.9%	51.4% : 24.3% : 24.3%	47.9% : 27.4% : 24.7%

C. Three-receiver System

An experimental three-receiver system is shown in Fig. 10 (a), in which TX uses the large coil and all the receivers, RX_i ($i = 1, 2, 3$), use the small ones [refer to Fig. 4 and Table I]. Again TX is fixed at (0,0,0). RX_2 and RX_3 are placed with coordinates of (125, $\pm\frac{5\pi}{6}$, -10), respectively, while RX_1 moves from (125, 0, 0) to (125, π, 0) along a circle of radius 125 mm. The coupling coefficients, k_{t1}(=0.090), k_{t2}(=0.062), k_{t3}(=0.062), and k_{23}=(0.018) are again constant due to the unchanged relative positions between TX and RX_i's. Note among the three receivers the z-axis position of RX_1 is different. The cross coupling coefficients k_{12} and k_{13} in different positions are measured by VNA and shown in Fig. 10(b). For each position, the efficiency can be calculated as

$$\eta = \frac{|S_{21}|^2 + |S_{31}|^2 + |S_{41}|^2}{1 - |S_{11}|^2}, \tag{36}$$

and the power division ratio is

$$P_1 : P_2 : P_3 = |S_{21}|^2 : |S_{31}|^2 : |S_{41}|^2. \tag{37}$$

Again, the S-parameters and $\mathbf{Z_{IN}}$ are measured by VNA [refer to Fig. 2].

When the loads are all pure resistive ones (the standard 50 Ω each), the system efficiency varies significantly in different positions. As shown in Fig. 11, for the uncompensated system the worst-case efficiency (78%) occurs again when RX_1 is rightly above RX_2, i.e., $\theta_1 = \frac{5\pi}{6}$ and a maximum k_{12}. k_{12} is a key factor between $\theta_1 = 0$ and $\theta_1 = \frac{5\pi}{6}$. After that, the influence of k_{13} becomes more obvious [refer to Fig. 10(b) and Fig. 11]. It is interesting to notice that at certain positions such as θ_1=$\frac{2\pi}{3}$ and π, the cross coupling between the receiving coils is actually cancelled. Thus the improvement of the system efficiency can be observed from $\theta_1 = \frac{5\pi}{6}$ to $\theta_1 = \pi$. Similar to the two-receiver system, the optimal load reactances are calculated and applied to compensate the cross coupling. Fig. 11 shows the compensation can significantly recover the decrease in the system efficiency as predicted by calculation. The efficiency is maintained around 88% at various positions of RX_1. The frequency responses when $\theta_1 = \frac{5\pi}{6}$ are given and compared in Fig. 12. Again the shift of the resonance frequency can be avoided after the compensation. In addition, the input impedance and power division ratio in the two extreme cases, $\theta_1 = 0$ and $\frac{5\pi}{6}$, are summarized and compared in Table III and IV. Note in the current three-receiver system, the cross coupling exists between RX_2 and RX_3 even θ_1 is zero. Similar results are obtained that show the proposed compensation can preserve not only the system efficiency but also the input impedance $\mathbf{Z_{IN}}$ and the power division ratio $P_1 : P_2 : P_3$ when there is cross coupling among the three receivers.

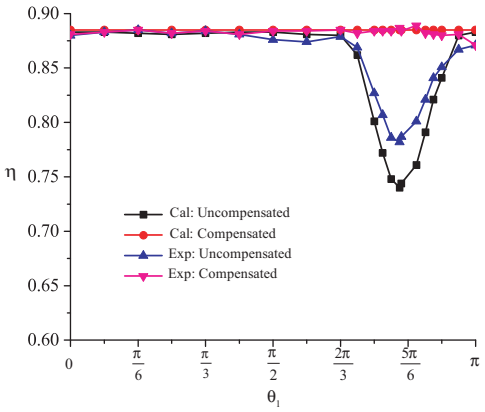

Fig. 11. Comparison of the system efficiencies in the three-receiver system.

It should be noted that apart from the mutual inductances, other parasitic effects such as mutual capacitances exist among overlapping coils [34]. The good agreement between the above experimental and calculated results indicates that these mutual capacitances do not play a significant role in the current experimental setup. Meanwhile, the basic trend is that the closer the distance between overlapping coils and higher the operating frequency, the more prominent the mutual capacitances would be [34], [35]. In such cases, the accuracy of the above circuit models of the multiple-receiver WPT systems could be affected. Alternative models must be developed that take into account for these additional mutual reactance effects.

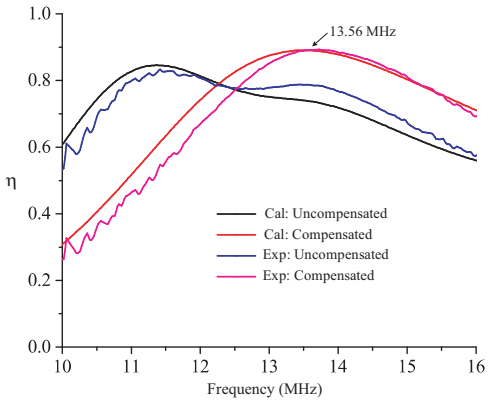

Fig. 12. Frequency responses of the three-receiver system at $\theta_1 = \frac{5\pi}{6}$.

V. Conclusion

In this paper a comprehensive theoretical analysis is carried out on the influence of the cross coupling and its compensation in multiple-receiver WPT systems. The optimal load reactances are analytically derived and verified for both the two-receiver systems and the general multiple-receiver systems. It shows that the decrease in the system efficiency due to the non-zero cross coupling can largely be recovered by having the optimal load reactances. The other important system characteristics such as the input impedance and power distribution can also be preserved. The results are validated by means of both the model-based calculation and the final experiments. Thus the validated theoretical analysis will serve as a key step in developing a design framework for future multiple-receiver, as well as multiple-transmitter, WPT systems. Based on the findings in this paper, further work could involve the development of a practical control scheme for an optimized power distribution in multiple-receiver WPT systems.

References

[1] S. Aldhaher, P. Luk, and J. Whidborne, "Tuning class E inverters applied in inductive links using saturable reactors," *IEEE Trans. Power Electron.*, vol. 29, no. 6, pp. 2969–2978, 2014.

[2] S. Aldhaher, P. Luk, A. Bati, and J. Whidborne, "Wireless power transfer using class E inverter with saturable dc-feed inductor," *IEEE Trans. Ind. Appl.*, vol. 50, no. 4, pp. 2710 – 2718, 2014.

[3] T. Imura and Y. Hori, "Maximizing air gap and efficiency of magnetic resonant coupling for wireless power transfer using equivalent circuit and neumann formula," *IEEE Trans. Ind. Electron.*, vol. 58, no. 10, pp. 4746–4752, 2011.

[4] A. P. Sample, D. A. Meyer, and J. R. Smith, "Analysis, experimental results, and range adaptation of magnetically coupled resonators for wireless power transfer," *IEEE Trans. Ind. Electron.*, vol. 58, no. 2, pp. 544–554, 2011.

[5] M. Budhia, G. A. Covic, and J. T. Boys, "Design and optimization of circular magnetic structures for lumped inductive power transfer systems," *IEEE Trans. Power Electron.*, vol. 26, no. 11, pp. 3096–3108, 2011.

[6] T. C. Beh, M. Kato, T. Imura, S. Oh, and Y. Hori, "Automated impedance matching system for robust wireless power transfer via magnetic resonance coupling," *IEEE Trans. Ind. Electron.*, vol. 60, no. 9, pp. 3689–3698, 2013.

[7] J. Park, Y. Tak, Y. Kim, Y. Kim, and S. Nam, "Investigation of adaptive matching methods for near-field wireless power transfer," *IEEE Trans. Antennas Propag.*, vol. 59, no. 5, pp. 1769–1773, 2011.

[8] M. Fu, C. Ma, and X. Zhu, "A cascaded boost-buck converter for high efficiency wireless power transfer systems," *IEEE Trans. Ind. Informat.*, vol. 10, no. 3, pp. 1972–1980, 2014.

[9] W. X. Zhong and S. Y. R. Hui, "Maximum energy efficiency tracking for wireless power transfer systems," *IEEE Trans. Power Electron.*, vol. 30, no. 7, pp. 4025–4034, 2015.

[10] M. Fu, H. Yin, X. Zhu, and C. Ma, "Analysis and tracking of optimal load in wireless power transfer systems," *IEEE Trans. Power Eletron.*, vol. 30, no. 7, pp. 3952–3963, 2015.

[11] D. Krschner and C. Rathge, "Maximizing dc-to-load efficiency for inductive power transfer," *IEEE Trans. Power Electron.*, vol. 28, no. 5, pp. 2437–2447, 2013.

[12] D. Ahn and S. Hong, "Wireless power transmission with self-regulated output voltage for biomedical implant," *IEEE Trans. Ind. Electron.*, vol. 61, no. 5, pp. 2225–2235, 2014.

[13] C.-Y. Huang, J. E. James, and G. A. Covic, "Design considerations for variable coupling lumped coil systems," *IEEE Trans. Power Electron.*, vol. 30, no. 2, pp. 680–689, 2015.

[14] W. Ni, I. B. Collings, X. Wang, R. P. Liu, A. Kajan, M. Hedley, and M. Abolhasan, "Radio alignment for inductive charging of electric vehicles," *IEEE Trans. Ind. Informat.*, vol. 11, no. 2, pp. 427–440, 2015.

[15] J. J. Casanova, Z. N. Low, and J. Lin, "A loosely coupled planar wireless power system for multiple receivers," *IEEE Trans. Ind. Electron.*, vol. 56, no. 8, pp. 3060–3068, 2009.

[16] A. Kurs, R. Moffatt, and M. Soljačić, "Simultaneous mid-range power transfer to multiple devices," *Applied Physics Letters*, vol. 96, no. 4, p. 044102, 2010.

[17] S. Lee, S. Kim, and C. Seo, "Design of multiple receiver for wireless power transfer using metamaterial," in *2013 Asia-Pacific Microwave Conference Proceedings (APMC), Seoul, Korea*, Nov. 2013, pp. 1036–1038.

[18] U. Azad and I. Tzanidis, "Resonant coupling efficiency limits for multiple receivers in a wireless power transfer system," in *2013 IEEE Antennas and Propagation Society International Symposium (APSURSI), Orlando, USA*, July 2013, pp. 846 – 847.

[19] A. K. Swain, S. Devarakonda, and U. K. Madawala, "Modeling, sensitivity analysis, and controller synthesis of multipickup bidirectional inductive power transfer systems," *IEEE Trans. Ind. Informat.*, vol. 10, no. 2, pp. 1372–1380, 2014.

[20] P. Riehl, A. Satyamoorthy, H. Akram, Y.-C. Yen, J.-C. Yang, B. Juan, C.-M. Lee, F.-C. Lin, V. Muratov, W. Plumb, and P. Tustin, "Wireless power systems for mobile devices supporting inductive and resonant operating modes," *IEEE Trans. Microw. Theory Tech.*, vol. 63, no. 3, pp. 780 – 790, 2015.

[21] J. Kim, D.-H. Kim, and Y.-J. Park, "Analysis of capacitive impedance matching networks for simultaneous wireless power transfer to multiple devices," *IEEE Trans. Ind. Electron.*, vol. 62, no. 5, pp. 2807 – 2813, 2015.

[22] X. Liu, C. Wuhan, G. Wang, and W. Ding, "Efficient circuit modelling of wireless power transfer to multiple devices," *IET Power Electron.*, vol. 7, no. 12, pp. 3017 – 3022, 2014.

[23] Y. Zhang, Z. Zhao, K. Chen, F. He, and L. Yuan, "Wireless power transfer to multiple loads over various distances using relay resonators," *IEEE Antennas Wireless Propag. Lett.*, vol. 25, no. 5, pp. 337 – 339, 2015.

[24] K. Lee, Kunsan, Kunsan, and D.-H. Cho, "Analysis of wireless power transfer for adjustable power distribution among multiple receivers," *IEEE Antennas Wireless Propag. Lett.*, vol. 14, pp. 950–953, 2015.

[25] L. J. Chen, J. T. Boys, and G. A. Covic, "Power management for multiple-pickup IPT systems in materials handling applications," *IEEE Journal of Eerging and Selected Topics in Power Electronics*, vol. 3, no. 1, pp. 163–176, 2015.

[26] B. L. Cannon, J. F. Hoburg, D. D. Stancil, and S. C. Goldstein, "Magnetic resonant coupling as a potential means for wireless power transfer to multiple small receivers," *IEEE Trans. Power Electron.*, vol. 24, no. 7, pp. 1819–1825, 2009.

[27] D. Ahn and S. Hong, "Effect of coupling between multiple transmitters or multiple receivers on wireless power transfer," *IEEE Trans. Ind. Electron.*, vol. 60, no. 7, pp. 2602–2613, 2013.

[28] K. K. Ean, B. T. Chuan, T. Imura, and Y. Hori, "Impedance matching and power division algorithm considering cross coupling for wireless power transfer via magnetic resonance," in *Proc. IEEE 34th International Telecommunications Energy Conference (INTELEC)*, Sep. 2012, pp. 1–5.

[29] C. K. Lee, W. Zhong, and S. Hui, "Effects of magnetic coupling of nonadjacent resonators on wireless power domino-resonator systems," *IEEE Trans. Power Electron.*, vol. 27, no. 4, pp. 1905–1916, 2012.

[30] W. Zhong, C. K. Lee, and S. Hui, "Wireless power domino-resonator systems with noncoaxial axes and circular structures," *IEEE Trans. Power Electron.*, vol. 27, no. 11, pp. 4750–4762, 2012.

[31] J. Kim, H.-C. Son, D.-H. Kim, and Y.-J. Park, "Impedance matching considering cross coupling for wireless power transfer to multiple receivers," in *2013 IEEE Wireless Power Transfer Conference (WPTC), Perugia, Italy*, May 2013, pp. 226–229.
[32] M. Fu, T. Zhang, C. Ma, and X. Zhu, "Efficiency and optimal loads analysis for multiple-receiver wireless power transfer systems," *IEEE Trans. Microw. Theory Tech.*, vol. 63, no. 3, pp. 801–812, 2015.
[33] Y. Lim, H. Tang, S. Lim, and J. Park, "An adaptive impedance-matching network based on a novel capacitor matrix for wireless power transfer," *IEEE Trans. Power Electron.*, vol. 29, no. 8, pp. 4403–4413, 2014.
[34] U. Jow and M. Ghovanloo, "Geometrical design of a scalable overlapping planar spiral coil array to generate a homogeneous magnetic field," *IEEE Trans. Magn.*, vol. 49, no. 6, pp. 2933–2945, 2013.
[35] E. J. Denlinger, "A frequency dependent solution for microstrip transmission lines," *IEEE Trans. Microw. Theory Tech.*, vol. 19, no. 1, pp. 30–39, 1971.

Minfan Fu (S'13-M'16) received the B.S. and M.S. degrees both in electrical and computer engineering from University of Michigan-Shanghai Jiao Tong University Joint Institute, Shanghai Jiao Tong University, Shanghai, China in 2010 and 2013, respectively, where he is currently working toward Ph.D. degree. His research interests include megahertz wireless power transfer, resonant converter, and circuit optimization.

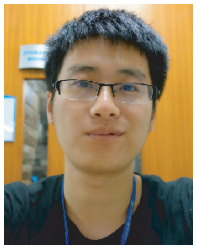

Tong Zhang received the B.S. and M.S. degree both in the electrical and computer engineering from University of Michigan-Shanghai Jiao Tong University Joint Institute, Shanghai, China in 2012 and 2015, respectively. Currently, he works as an engineer in Intel Asia-Pacific Research & Development Limited, Shanghai, China. His research interests include the coupling system analysis and the circuit design for wireless power transfer.

Xinen Zhu (S'04-M'09) received the B.Eng. (Hons.) degree in electronic and communication engineering from City University of Hong Kong, Hong Kong, in 2003, and the M.S. degree and the Ph.D. degree in electrical engineering from The University of Michigan at Ann Arbor, in 2005 and 2009 respectively. He is currently a tenure-track assistant professor of electrical and computer engineering with the University of Michigan-Shanghai Jiao Tong University Joint Institute, Shanghai Jiao Tong University, Shanghai, China. His research interests include wireless power transfer, tunable RF/microwave circuits, and ferroelectric thin films.

Patrick Chi-Kwong Luk (M'92-SM'08) was born in Hong Kong. He received the High Diploma with merits (BSc) in electrical engineering from The Hong Kong Polytechnic University (PolyU), Hong Kong, in 1983, the M.Phil degree in electrical engineering from Sheffield University, U.K., in 1989, and the Ph.D degree in electrical engineering from the University of South Wales in 1992. He started his career in industry as Engineer Trainee between 1981-83 at GEC (H.K.) and then after graduation as Applications Engineer at Polytek Engineering Co. (H.K.). In 1986, he worked as Senior Researcher in the Industrial Centre, PolyU. Since 1988, he had held academic positions at the University of South Wales, Robert Gordon University, Aberdeen, U.K., and University of Hertfordshire, U.K. He joined Cranfield University, U.K., in 2002, where he is a Chair Professor in Electrical Engineering and Head of the Electric Power and Drives Group in the School of Engineering. He sits in several IEEE Committees on Electrical Machines and is the Chairman of the IEEE UKRI Young Professionals. He is also an Associate Editor for IEEE Transactions on Power Electronics, IEEE Transactions on Smart Grids, and IET Renewable Power Generation. He has over 160 publications and co-holder of several patents in power electronics, motor drives, and control. His current research interests include electrical drives, renewable energy systems, and high-frequency power electronics. In 2014, he was supported by the Top Notch Foreign Specialist Program as a visiting professor at Shanghai Jiao Tong University in China.

Chengbin Ma (M'05) received the B.S.E.E. (Hons.) degree from East China University of Science and Technology, Shanghai, China, in 1997, and the M.S. and Ph.D. degrees both in the electrical engineering from University of Tokyo, Tokyo, Japan, in 2001 and 2004, respectively. He is currently a tenure-track assistant professor of electrical and computer engineering with the University of Michigan-Shanghai Jiao Tong University Joint Institute, Shanghai Jiao Tong University, Shanghai, China. He is also with a joint faculty appointment in School of Mechanical Engineering, Shanghai Jiao Tong University. Between 2006 and 2008, he held a post-doctoral position with the Department of Mechanical and Aeronautical Engineering, University of California Davis, California, USA. From 2004 to 2006, he was a R&D researcher with Servo Laboratory, Fanuc Limited, Yamanashi, Japan. His research interests include wireless power transfer, networked hybrid energy systems, and mechatronic control.